Comparing two mechanistic formalisms for soil organic matter dynamics: A test with in vitro priming effect observations

Cathy Neill, Bertrand Guenet

Soil Biology & Biochemistry 42 (2010) 1212–1221

Contents lists available at ScienceDirect

Soil Biology & Biochemistry

journal homepage: www.elsevier.com/locate/soilbio

Comparing two mechanistic formalisms for soil organic matter dynamics: A test with in vitro priming effect observations

Cathy Neill*, Bertrand Guenet

Université Pierre et Marie Curie, Laboratoire Biogéochimie et Ecologie des Milieux Continentaux, UMR 7618 CNRS/Paris 6, 46 rue d'Ulm, 75230 Paris Cedex 05, France

ARTICLE INFO

Article history:
Received 29 January 2010
Received in revised form
16 April 2010
Accepted 21 April 2010
Available online 7 May 2010

Keywords:
Model comparison
Maximum caliber
Organic matter dynamics
Litter decomposition
Mineral nitrogen
Microbial biomass
^{13}C labelling
Priming effect

ABSTRACT

First order kinetics characterize most models of soil organic matter dynamics. Although first order kinetics often provide a good description of litter decomposition, their general applicability has recently been challenged by numerous observations of priming effects. A priming effect can be defined as a change in native soil organic matter decomposition rate following the addition of some labelled exogenous substrate. Recently two new formalisms were developed which predict a priori the existence of priming effects, whether positive or negative. The Extended Mass Action (EMA) formalism is a generalization of enzyme kinetics at the microbial scale. The Maximum Caliber (MAXCAL) formalism describes the most probable dynamics of a system that arises when the multiple ways feasible macroscopic dynamics can be realized at the microscopic particle scale are accounted for. Here those two formalisms were applied to a common soil compartimentation scheme and their predictions confronted with an appropriate set of priming observations. We show that the two formalisms generate distinct, testable predictions and that the MAXCAL formalism performed better than the EMA formalism. We discuss the determinants of priming effects as predicted by the Maximum Caliber formalism.

1. Introduction

Soil organic matter performs a number of key functions in agroecosystems. It is a major reservoir of nutrients for plants. It also maintains an aggregated soil structure enabling water and air movement in soils. On a global scale, soil carbon is an important pool as well. It is a quantitatively important pool (approx. twice the atmospheric carbon pool (Schlesinger and Andrews, 2000)), and has proven sensitive enough to global changes to represent either a significant carbon sink or source (Guo and Gifford, 2002; Paul et al., 1997; Lal et al., 1995).

Our current understanding of soil organic matter dynamics is synthesized and quantitative predictions made possible with the help of mathematical models. Soil organic matter models are numerous (reviewed in Manzoni and Porporato, 2009). They usually differ in the way they partition soil organic matter into compartments (or "fractions"). However, many of them, including the popular Century model (Parton et al., 1987), share a common mathematical formalism, namely first order kinetics.

First order kinetics assume that the decomposition rate of some organic fraction is proportional to the amount of carbon in that fraction (although some nitrogen limitation may be included based on microbial stoichiometric requirements for N).

Despite the consensus on the robustness of these kinetics reflected by current models, first order kinetics are questionable. They indeed fail to account for organic matter dynamics as observed with isotope labelling and tracing. Short to medium-term incubations of soil samples amended with ^{14}C or ^{13}C labelled substrates have consistently shown that decomposition processes of distinct substrates interact with one another (reviewed in Blagodatskaya and Kuzyakov, 2008; Kuzyakov et al., 2000). Adding some labelled substrate may suppress or enhance native (unlabelled) soil organic matter mineralization. This phenomenon, known as the priming effect – whether positive or negative – seemingly contradicts first order kinetics. Indeed first order kinetics entail no interactions between the decomposition processes of distinct substrates.

As priming effects may be quantitatively important at the yearly scale and perhaps even more so if their cumulative effects are considered on the long run (e.g. Fontaine et al., 2004a, 2007), the following questions arise: How can we model them? What would

* Corresponding author at: Present address: Bioemco, Centre INRA Versailles-Grignon, Bâtiment Eger, 78850 Thiverval-Grignon, France. Tel.: +33 1 30 81 59 58; fax: +33 1 30 81 54 97.
E-mail addresses: neill@biologie.ens.fr (C. Neill), guenet@biologie.ens.fr (B. Guenet).

0038-0717/$ – see front matter © 2010 Elsevier Ltd. All rights reserved.
doi:10.1016/j.soilbio.2010.04.016

be the consequences for long-term kinetics? Should we change our current modelling consensus about first order kinetics?

Recently Neill and colleagues developed a new modelling approach to ecosystem dynamics (Neill and Gignoux, 2008; Neill et al., 2009). This approach is applicable to soil systems as well. It is a combinatorial approach that consists in calculating the trajectory of a system that is most probable because it can be realized in more ways at the individual "particle" scale (whether particles of matter or living particles). The number of ways a trajectory can be realized at a microscopic scale has been coined the "caliber" by Jaynes (1985). The model predicts that a system will follow its maximum caliber trajectory.

When applied to a soil system consisting of labelled and unlabelled organic fractions, and one explicit microbial pool, the maximum caliber ("MAXCAL") formalism predicts a priori the existence of positive and negative priming effects as the result of two antagonistic mechanisms: on the one hand, native soil organic matter mineralization is an increasing function of microbial biomass, which may increase if fed by the added substrate; on the other hand, native soil organic matter mineralization is a decreasing function of the availability of other substrates, because substrates compete with one another to be decomposed by microbes. If microbes have a higher affinity for the added substrate, they will utilize it preferentially and this may induce a negative priming effect.

An alternate formalism that can produce positive and negative priming effects has been offered by Neill and Gignoux (2006). This formalism can be derived from an analogy between decomposition processes and enzymatic reactions, using the law of mass action. Neill and Gignoux (2006) showed that it generalizes well-known formalisms such as the Michaelis–Menten formalism, its inverse, or the Beddington-DeAngelis formalism (Beddington, 1975; DeAngelis et al., 1975). We will call it the "extended mass action" formalism, "EMA" in short.

The two formalisms, MAXCAL and EMA, are in fact intriguingly similar, but they do differ in some important aspects, and are derived from entirely different rationales. It seemed interesting to compare them and rate them with quantitative data on priming effects. To do so, we used a series of incubations of cultivated soils amended with various amounts of ^{13}C labelled wheat straw and mineral nitrogen (Guenet et al., submitted). This paper reports the results of this model comparison.

2. Model description and methods

2.1. The data

To test the two formalisms, we used a series of 80 day in vitro soil incubations that are described and discussed in detail elsewhere (Guenet et al., submitted). Briefly, the soil used was a cultivated soil from Paris area, France (C:N ratio of 10, 10.4 g C/kg soil). 20 g soil samples were incubated at constant temperature (20 °C) and humidity (pF 2.75) in 120 mL flasks. The experiment followed a 4 × 3 incomplete factorial design, the first factor being the addition of ^{13}C labelled wheat straw (C:N ratio of 44) and the second factor the final C:N ratio of exogenous inputs (the latter being manipulated by additions of mineral nitrogen), yielding a total of nine treatments plus one control. Table 1 sums up the various amounts added. For instance treatment C1N1 corresponded to an addition of 1.5 g C straw per kg soil and 16 mg mineral nitrogen, which, including the nitrogen content of the straw, yielded a final input C:N ratio of 30. ^{13}C labelled and unlabelled CO_2 respiration were measured throughout the incubation period. In all, 15 replicates per treatment were set up, permitting the destructive harvest of three of the replicates on incubation days 3, 7, 15, 28 and 80 for mineral nitrogen concentration measurements. Figs. 1, 2 and 3 show the dynamics of cumulated labelled and unlabelled CO_2 and mineral nitrogen concentration respectively.

Table 1
Experimental treatments.

Treatment Name	Straw added (gC kg^{-1} soil)	Mineral nitrogen added (gN kg^{-1} soil)	Final input C:N ratio
Control C0N0	0	0	n.a.
C1N0	1.5	0	44
C2N0	2.2	0	44
C3N0	3.2	0	44
C1N1	1.5	0.016	30
C2N1	2.2	0.0235	30
C3N1	3.2	0.0346	30
C1N2	1.5	0.0395	20
C2N2	2.2	0.0581	20
C3N2	3.2	0.0854	20

2.2. The model structure

The comparison of the two formalisms required a common model structure upon which both formalisms could be applied. We chose the simplest model structure to represent the incubated soils, namely one native, unlabelled soil organic matter pool (hereafter denoted humus because soil was collected at depth >5 cm and sieved to remove most fresh plant residues), one ^{13}C labelled wheat straw pool (denoted litter), one microbial pool and one mineral nitrogen pool (Fig. 4). This parsimonious choice had advantages and drawbacks. On the one hand, successful predictions stemming from a simple model structure gives more credit to the mathematical formalism applied upon that structure, whereas positive results obtained with an over-parameterized model are difficult to interpret. On the other hand, an overly simple model structure can jeopardize the ability of the formalism to account for the data. We will return to this issue below.

With this model structure, we assumed three microbial fluxes would govern the dynamics of the whole system: microbial growth on humus, x_h, microbial growth on litter, x_l, and microbial mortality z. We assumed those three fluxes would determine all the other fluxes through stoichiometric relationships (Fig. 4), so that the dynamics of the system could be described by the following equations:

$$\delta c_h = -\nu_h x_h + \eta z \quad (1)$$

$$\delta c_l = -\nu_l x_l \quad (2)$$

$$\delta b = x_h + x_l - z \quad (3)$$

$$\delta n = (n_h \nu_h - n_b) x_h + (n_b - \eta n_h) z - (n_b - n_l \nu_l) x_l \quad (4)$$

where c_h, c_l, b and n stand for humus carbon, litter carbon, microbial biomass carbon and mineral nitrogen respectively and the symbol δ denotes their variation over a small time step δt (Table 2 sums up the model parameters and state variables). Units chosen for c_h, c_l and b were gC per kg of soil, and gN per kg of soil for n. Eq. (1) says that for any new microbial unit grown on humus, ν_h humus units have been decomposed (and thus $\nu_h - 1$ units have been mineralized to CO_2). Likewise ν_l denotes the number of litter units needed to make up one new microbial unit. When c_h, c_l and b are expressed in gC per kg soil, ν_h and ν_l can be viewed as inverse of carbon assimilation yields. Next, for any microbial unit that dies, a fraction η of it is humified and thus feeds the humus stock. The rest is mineralized to CO_2, accounting in particular for maintenance respiration.

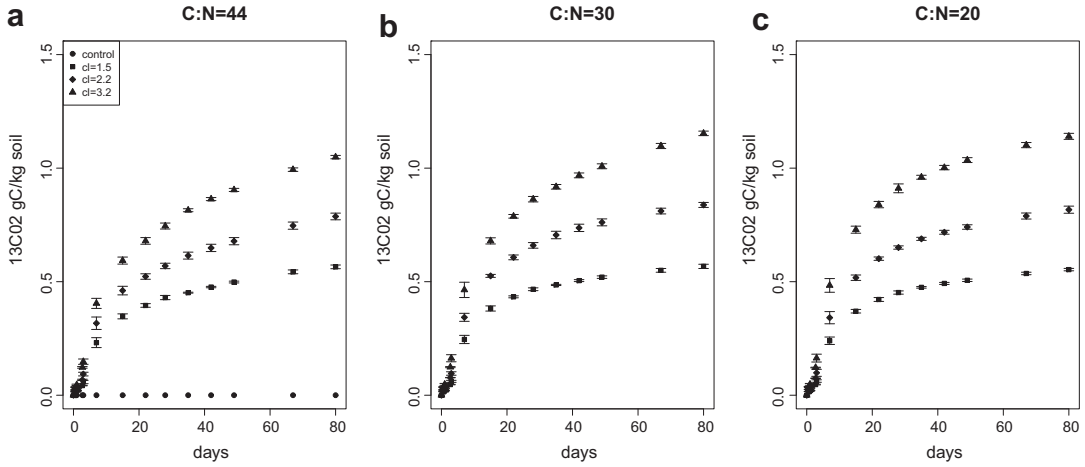

Fig. 1. Cumulated ^{13}C labelled CO_2 respiration for all treatments. Each panel corresponds to a different exogenous input C:N ratio (44 (a), 30 (b), 20 (c)). Within a panel, different symbols correspond to different straw supply levels (in gC per kg soil): 0 (circles), 1.5 (squares), 2.2 (diamonds), 3.2 (triangles).

Nitrogen dynamics are a little bit more complicated. Let n_h denote the nitrogen concentration of humus and n_b that of microbes. Microbial growth on humus is accompanied with a gross immobilization flux $n_b x_h$. Nitrogen is supplied by humus decomposition itself, up to $n_h \nu_h x_h$. This usually results in excess nitrogen compared to microbial demand, yielding a net mineralization rate $(n_h \nu_h - n_b) x_h$. In contrast, growth on litter should result in a net immobilization rate $(n_b - n_l \nu_l) x_l$ because gross mineralization from litter decomposition $n_l \nu_l x_l$ does not meet microbial requirements $n_b x_l$. Finally microbial mortality offers $n_b z$ units of nitrogen while humification with concentration n_h requires $n_h \eta z$ nitrogen units. We checked that we always had $n_b \geq \eta n_h$ so that there would be no requirements of mineral nitrogen for humification (which would have implied a functional dependency of microbial turnover on mineral nitrogen availability, an unlikely outcome). These mass balance equations and in particular this representation of microbial stoichiometric constraints is not new and in fact similar to many models (e.g. Molina, 1996; Agren and Bosatta, 1996) see (Manzoni and Porporato, 2009).

We can also write mass balance equations governing the variations of cumulated CO_2 respiration coming from the unlabelled and ^{13}C labelled carbon pools respectively. We will denote those cumulated respirations w_{12} and w_{13} respectively, and we have :

$$\delta w_{12} = (1 - a_h)(\nu_h - 1)x_h + (1 - a_l)(\nu_l - 1)x_l + (1 - a_z)(1 - \eta)z \quad (5)$$

$$\delta w_{13} = a_h(\nu_h - 1)x_h + a_l(\nu_l - 1)x_l + a_z(1 - \eta)z \quad (6)$$

where a_h, a_l and a_z respectively refer to the ^{13}C labelled fraction $((labelled)/(unlabelled + labelled)\ fraction)$ of the fluxes x_h, x_l and z. Let a_{c_h}, a_{c_l} and a_b stand for the ^{13}C labelled fractions of humus, litter and microbial biomass respectively. We have $a_{c_l} = 1$ at all times and $a_{c_h} = 0$ at time zero. Throughout the analysis, we assumed that $a_{c_h} \approx 0$ (i.e. the labelling of humus by litter humification was negligible, which can be checked with simulations). We also assumed $a_h \approx a_{c_h}$ and $a_l \approx a_{c_l}$. This last assumption means that the isotopic signature of microbial biomass does not affect the signature of the litter or humus mineralization fluxes. Alternatively we could have assumed for instance that $a_l = (\nu_l a_{c_l} + a_b)/(\nu_l + 1)$, i.e. the microbial signature dilutes that of litter. This can generate an apparent priming effect where the unlabelled carbon of microbial biomass is respired as a result of litter decomposition. However, in such a model, as microbial biomass becomes labelled by litter decomposition, its dilution effect fades out and the reverse phenomenon appears: humus mineralization becomes labelled by

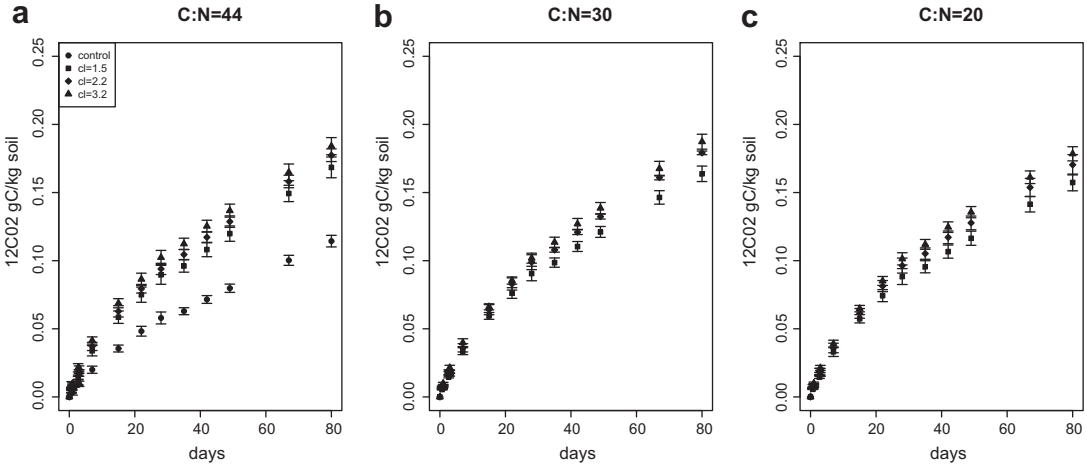

Fig. 2. Cumulated unlabelled CO_2 respiration for all treatments. Legend same as Fig. 1.

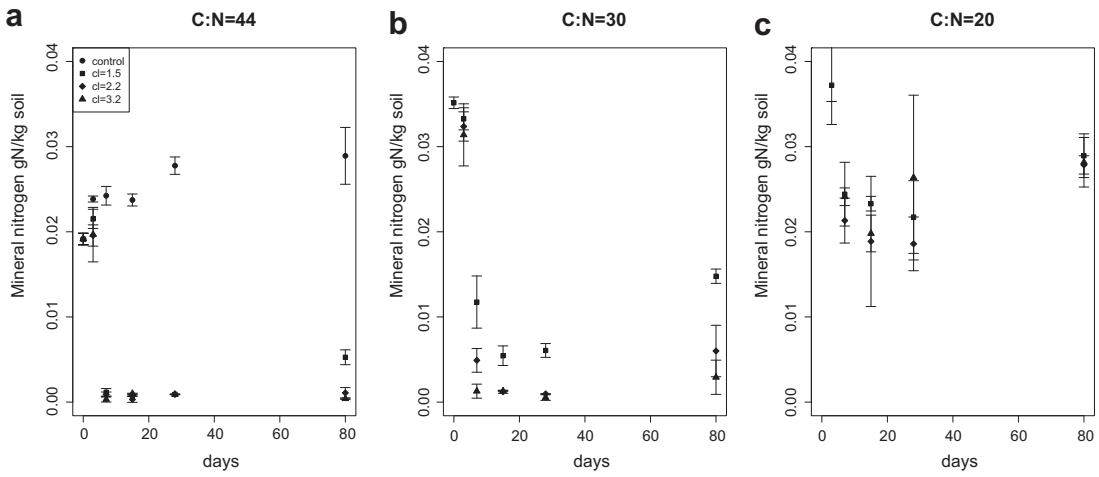

Fig. 3. Mineral nitrogen concentration time courses. Legend same as Fig. 1.

labelled biomass as well. We noticed that the two phenomena cancelled out in model simulations, resulting in no apparent priming. Moreover, the data shows no evidence of an apparent priming in the first days of the incubation (Fig. 2). Therefore we decided to neglect this phenomenon and assumed $a_h = 0$ and $a_l = 1$. Finally we also assumed that unlabelled biomass varied little throughout the incubations, compared to labelled biomass. This is supported by the data itself, as any abrupt change in unlabelled biomass should have been reflected in the unlabelled CO_2 respiration which fuels it (Fig. 2). Direct biomass measurements in other priming experiments also support this hypothesis (N. Nunan, pers. comm. and Fontaine et al., 2004b). Near steady state for unlabelled biomass implies that $(1 - a_z)z \approx x_h$, i.e. $a_z z \approx z - x_h$.

With these assumptions, eqs. (5) and (6) become:

$$\delta w_{12} = (\nu_h - \eta)x_h \tag{7}$$

$$\delta w_{13} = (\nu_l - 1)x_l + (1 - \eta)(z - x_h) \tag{8}$$

Together with eq. (4), one can see that x_h, x_l and z are linearly related to δw_{12}, δw_{13} and δn. This remains true if the fluxes are cumulated over any given time interval. These equations can help us link the actual measurements made on larger time steps Δt (Δw_{12}, Δw_{13} and Δn) with the underlying fluxes cumulated over the same Δt. To distinguish "instantaneous" fluxes (i.e. calculated on δt) x_h, x_l and z from cumulated ones, we will denote the latter with capital letters X_h, X_l and Z.

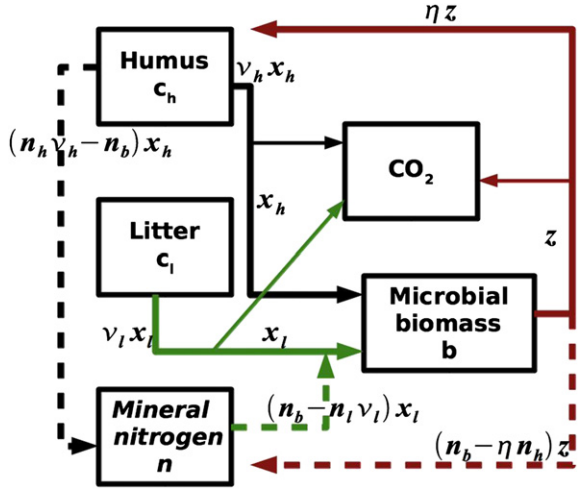

Fig. 4. Model structure.

2.3. The formalisms

The mass balance equations described above do not suffice to complete a soil organic matter model. Mathematical formalisms are needed to calculate the fluxes x_h, x_l and z as a function of the state variables c_h, c_l, b and n. We considered two alternate formalisms applying on small but discrete time steps. We chose discrete time steps because we knew that the MAXCAL formalism could only apply on discrete time steps (due to its conceptual framework), while the EMA formalism is likely flexible. The extended mass action formalism offered in Neill and Gignoux (2006) is based on an analogy with enzyme kinetics at the microbial cell scale. It is derived from the law of mass action and mass conservation constraints, with no simplifying assumptions as in standard enzyme kinetics. When applied to the framework developed here, this formalism reads:

$$x_h = k_h(b - x_h - x_l - z)\left(\frac{c_h - \nu_h x_h}{\nu_h}\right) \tag{9}$$

$$x_l = k_l(b - x_h - x_l - z)\left(\frac{c_l - \nu_l x_l}{\nu_l}\right)\left(\frac{n - \nu_n x_l}{\nu_n}\right) \tag{10}$$

$$z = m(b - x_h - x_l - z) \tag{11}$$

where k_h, k_l, m are kinetic constants and $\nu_n = n_b - n_l \nu_l$. It is easy to show that when $x_l = 0$, and $c_h/\nu_h \gg b$(resp. $b \gg c_h/\nu_h$), eq. (9) reduces to $x_h = k_h(bc_h/\nu_h)/(1 + k_h c_h/\nu_h)$(resp. $x_h = k_h(bc_h/\nu_h)/(1 + k_h b)$), a formalism which is similar to the Michaelis–Menten formalism (resp. its inverse). Alternatively, when $x_l = 0$ and either b or $c_h/\nu_h \ll 1/k_h$ then eq. (9) reduces to $x_h = k_h(bc_h/\nu_h)/(1 + k_h(b + c_h/\nu_h))$, a formalism analogous to the Beddington-DeAngelis formalism (Beddington, 1975; DeAngelis et al., 1975).

The MAXCAL formalism gives the most probable fluxes to be observed given energy and mass constraints, and given also the fact that any set of values for the three fluxes x_l, x_h and z can be the result of many different combinations of events at the microscopic level (indeed a particular microbial unit can be decomposing this particular humus unit or that other one). To better understand this

Table 2
Model variables and parameters summary. ad. stands for adimensional.

Model variable or parameter	Meaning	Unit	Value at day 0
c_h	Soil humus stock	gC kg^{-1} soil	10.4
c_l	Litter stock	gC kg^{-1} soil	1.5, 2.2 or 3.24
b	Microbial biomass	gC kg^{-1} soil	n.a.
n	Mineral nitrogen stock	gN kg^{-1} soil	0.0195 in the control + additions
w_{12}	Cumulated unlabelled CO_2 respiration	gC kg^{-1} soil	0
w_{13}	Cumulated labelled CO_2 respiration	gC kg^{-1} soil	0
a_x	^{13}C labelled fraction of a compartment or a flux	ad.	n.a.
x_h	Microbial growth on humus	gC kg^{-1} soil h^{-1}	n.a.
x_l	Microbial growth on litter	gC kg^{-1} soil h^{-1}	n.a.
z	Microbial decay	gC kg^{-1} soil h^{-1}	n.a.
ν_h	Number of humus units needed to make up one new microbial unit	ad.	2
ν_l	Number of litter units needed to make up one new microbial unit	ad.	1/0.6
ν_n	Number of mineral nitrogen units needed to make up one new microbial unit	ad.	$n_b - n_l\nu_l$
η	Microbial biomass humification coefficient	ad.	0.33–0.66
n_h	Humus nitrogen content	gN g^{-1} C humus	0.093
n_l	Litter nitrogen content	gN g^{-1} C litter	0.023
n_b	Microbial biomass nitrogen content	gN g^{-1} C biomass	1/12-1/8
k_h	Kinetic parameter for microbial growth on humus	ad.	n.a.
k_l	Kinetic parameter for microbial growth on litter	ad.	n.a.
m	Kinetic parameter for microbial decay	ad.	n.a.
δ	Indicates variations over a small time step δt compatible with the hypotheses of both formalisms	n.a.	n.a.
Δ	Indicates variations over a larger time step Δt	n.a.	n.a.

rationale, we refer the reader more specifically to the Neill et al. (2009) paper, where a simple example is fully worked out. The equations predicted by the maximum caliber approach read (Neill and Gignoux, 2008; Neill et al., 2009):

$$x_h = k_h(b - x_h - x_l - z)^{1/(1+\nu_h)}\left(\frac{c_h - \nu_h x_h}{\nu_h}\right)^{\nu_h/(1+\nu_h)} \quad (12)$$

$$x_l = k_l(b - x_h - x_l - z)^{1/(1+\nu_l+\nu_n)}\left(\frac{c_l - \nu_l x_l}{\nu_l}\right)^{\nu_l/(1+\nu_l+\nu_n)} \left(\frac{n - \nu_n x_l}{\nu_n}\right)^{\nu_n/(1+\nu_l+\nu_n)} \quad (13)$$

$$z = m(b - x_h - x_l - z) \quad (14)$$

where k_h, k_l, m are kinetic constants as well and again $\nu_n = n_b - n_l\nu_l$. These equations are implicit and have to be solved for x_h, x_l and z numerically when needed.

A fundamental assumption of the MAXCAL derivation and that must apply for EMA to be valid as well is that the time step δt be small enough that the total amount of each entity (c_h, c_l, b and n) involved in the fluxes x_h, x_l and z does not exceed the amount available at the beginning of the time step. This is equivalent to saying that newly formed items of each entity during δt will not participate to the fluxes during δt. Mass conservation then implies that $x_h + x_l + z \leq b$, $\nu_h x_h \leq c_h$, $\nu_l x_l \leq c_l$ etc. This also results in numerical stability for both formalisms.

One can show that the solutions of eqs. (12)–(14) verify $\partial x_h/\partial c_l < 0$ and $\partial x_h/\partial b > 0$ (see Appendix). This is the mathematical embodiment of the two priming mechanisms alluded to in the introduction: the first inequality expresses substrate competition and the second one mineralization enhancement upon biomass increase. The possibility of a negative priming in the EMA formalism has been shown numerically before (Neill and Gignoux, 2006).

The MAXCAL equations only differ from the EMA formalism in that the terms of the right hand side are raised to powers. In the MAXCAL formalism the sum of the exponents of the right hand side is always 1. As a result the corresponding kinetic constants are adimensional. In the EMA formalism, the dimension of kinetic constants varies with the number of reactants involved in the process.

2.4. Methods for model comparison

Preliminary data analysis suggested that (i) microbial C:N ratio varied between treatments (because the ratio (N immobilized in treatment + N mineralized in control)/(^{13}C mineralized in treatment) did, (Guenet et al., submitted for publication) and (ii) the kinetic constant k_l associated with the litter decomposition process (eq. (10) or 13) decreased with time within any given treatment. That is, as labile compounds of litter were mineralized, litter recalcitrance increased. As a result of (ii), neither formalisms could satisfactorily simulate the kinetics of litter mineralization with a constant value for k_l. In other words eqs. (10) and (13) were of little use here. We assumed however that humus and microbial characteristics were constant enough within each treatment for eqs. (9), (11), (12) and (14) to hold. That is, we assumed both formalisms were adequate to model x_h as a function of x_l and microbial turnover z. Specifically, using eqs. (12) and (14), the maximum caliber formalism predicts.

$$x_h = k_h\left(\frac{z}{m}\right)^{\frac{1}{1+\nu_h}}\left(\frac{c_h - \nu_h x_h}{\nu_h}\right)^{\frac{\nu_h}{1+\nu_h}}$$

With $c_h \gg x_h$, and c_h not varying significantly over the incubation period, this approximates to:

$$x_h \propto z^{\frac{1}{1+\nu_h}}$$

For the extended mass action formalism, we can derive a similar relationship:

$$x_h \propto z$$

Therefore both formalisms predict that the relationship $\log(x_h) \sim \log(z)$ should be linear, but they do not predict the same slope. These relationships hold for cumulated fluxes X_h and Z as well if x_h and z remain roughly constant during Δt. CO_2 respiration rates could be assumed constant between two consecutive measurements throughout the incubation period. In contrast,

substantial changes in mineral nitrogen concentrations occurred between days 0 and 15 with too few measurements having been done in this interval. But from day 15 onward, mineral nitrogen concentrations varied little in all treatments (Fig. 3). In the analyses we thus restricted the calculations of X_h and Z to days 15–67 and assumed mineral nitrogen concentrations remained at quasi-steady state ($\delta n \approx 0$) on that period for all treatments.

We calculated X_h and Z from actual measurements using only the stoichiometric linear system defined by eqs. (4), (7) and (8). We then sought to estimate the parameters β_0, β_1 of the regression $\log(X_h) = \log(\beta_0) + \beta_1 \log(Z)$, check the linearity of this relationship and test which formalism would best predict the slope β_1.

X_h and Z could be calculated using eqs.(4), (7) and (8) provided that all the stoichiometric parameters were known (including their variations among treatments). n_h and n_l had been measured; as noted before (Agren and Bosatta, 1996; Manzoni et al., 2008), the kind of data and mass balance equations used here do not constrain microbial assimilation yields and N:C ratio independently. Only critical ratios ν_l/n_b and ν_h/n_b are likely important to know. As microbial assimilation yields seem to vary less than microbial N:C ratios, ν_h and ν_l were assigned the values 2 and 1/0.6 respectively (recall that they are inverse of carbon assimilation effciencies) (Table 2). Finally, n_b and η were sufficiently uncertain and/or variable that we had to account for this in the analysis. We thus sought to estimate the Bayesian posterior distribution for the regression parameters $\beta = (\beta_0, \beta_1)$ ($\log(\beta_0)$ intercept and β_1 slope) and the correlation coefficient r of the $\log(X_h) \sim \log(Z)$ relationship as :

$$p(\beta, r/data) = \int_{\eta,n_b} p(\beta, r/\eta, n_b, data)p(\eta, n_b)d\eta dn_b$$

The sampling algorithm of $p(\beta, r/data)$ is detailed in the Appendix. Briefly, marginalizing over η and n_b required defining their plausibility distribution $p(\eta, n_b)$. We assumed η would be constant among treatments but could take any value within the interval [1/3, 2/3], following previous experimental (Kindler et al., 2006) and modelling results (Saffih-Hdadi and Mary, 2008; Nicolardot et al., 2001). We assumed n_b would vary among treatments in a systematic way (but would remain constant with time for any given treatment) so that knowing n_b in any one of the treatments allowed to assess n_b in all the other treatments. We describe this calculation in the Appendix. We assumed n_b in the treatment C1N0 could take any value within the [1/12, 1/8] interval, following global patterns in microbial C:N ratios (Cleveland and Liptzin, 2007). Hereafter n_b always refers to its value in the C1N0 treatment. For any given pair of values for η and n_b, we calculated all the cumulated fluxes X_h and Z between two consecutive respiration measurements between days 15 and 67 (those fluxes were normalized on a per day basis). We pooled all those fluxes into a single data set since neither formalisms predicted differences in the parameters of the $\log(X_h) \sim \log(Z)$ relationship among treatments. We neglected the uncertainty in those fluxes resulting from the uncertainty of the measurements, because we assumed most of the uncertainty in the regression parameters would come from the variance among treatments, not that within treatments. We sampled the posterior $p(\beta, r/data)$ and calculated the means and 95% confidence intervals for the regression parameters β and the correlation coefficient r.

3. Results

Table 3 shows the means and 95% confidence intervals of the posterior distribution of the regression parameters β and the correlation coefficient r. We also show the intervals spanned by the microbial C:N ratios in the various treatments, as calculated according to the methods for each pair of parameters η and n_b in treatment C1N0.

Table 3
Posterior mean (and 95% confidence intervals) for the regression parameters of the relationship $\log(X_h) \sim \log(Z)$, the correlation coefficient between those two variables and the microbial C/N ratios calculated for each treatment (marginalized over the probability density functions for η and n_b in treatment C1N0).

Model parameter	Posterior mean ± standard deviation
intercept log β_0	−4.7 ((−5.1)–(−4.25))
slope β_1	0.36 (0.32–0.39)
correlation coefficient r	0.93 (0.92–0.94)
$1/n_b$ in C1N0	9.8 (8.0–11.9)
$1/n_b$ in C2N0	11.4 (9.6–13.5)
$1/n_b$ in C3N0	13.2 (11.2–15.1)
$1/n_b$ in C1N1	8 (6.4–10)
$1/n_b$ in C2N1	8.2 (6.5–10.1)
$1/n_b$ in C3N1	8.4 (6.8–10.4)
$1/n_b$ in C1N2	7.1 (5.5–8.9)
$1/n_b$ in C2N2	6.5 (5–8.2)
$1/n_b$ in C3N2	6.4 (5–8.2)

With the prior intervals chosen for η and n_b in C1N0, microbial C:N ratios in other treatments remained within plausible values of 5 and 15 (Cleveland and Liptzin, 2007; Sterner and Elser, 2002). Also microbial C:N ratios varied consistently with the treatment input C:N ratios: they were similar among treatments with similar input C:N ratios and decreased with input C:N ratios. This agrees both with estimates provided in Guenet et al. (submitted for publication) and with previous statements that the microbial community evolves in such a way as to adjust its C:N ratio with the C:N ratio of its substrates (Danger et al., 2008) and lends support to our calculatory hypotheses.

The correlation coefficient r of the $\log(X_h) \sim \log(Z)$ relationship was superior to 0.9 with probability >0.975, indicating a linear relationship, as predicted by both formalisms (EMA and MAXCAL). As an illustration, Fig. 5 shows this relationship for $\eta = 0.5$ and $n_b = 0.1$ in C1N0.

The slope of this relationship β_1 had a mean value of 0.36 and a 95% confidence interval of 0.32–0.39. This is at odds with the predictions of the EMA formalism. In contrast, it agrees well with the predictions of MAXCAL: the latter predicts a slope equal to $1/(1+\nu_h)$, where ν_h is the inverse of the carbon assimilation yield for humus. With the value $\nu_h = 2$ that we have used throughout the calculations, the MAXCAL formalism thus predicts a slope of 1/3, which is very close to the observed mean and within the 95% confidence interval.

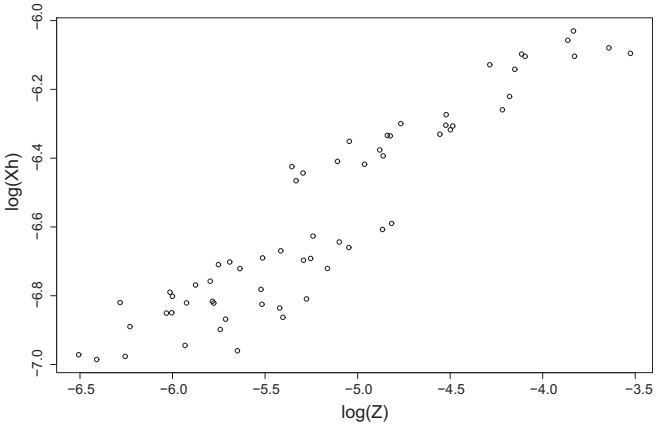

Fig. 5. $\log(X_h) \sim \log(Z)$ relationship, all treatments pooled, for $\eta = 0.5$ and $n_b = 0.1$ in C1N0. Values correspond to fluxes expressed in g C per kg soil per day.

The formalism comparison therefore supports the MAXCAL formalism over the EMA one.

Within the MAXCAL formalism, it can easily be shown identifying eqs. (12) and (14) with $x_h = \beta_0 z^{\beta_1}$ that i) $\beta_0 = ((k_h)/(m^{1/(1+\nu_h)}))(c_h/\nu_h)^{\nu_h/1+\nu_h}$ and ii) in a system with humus alone, x_h tends towards the value $x_h^0 = \beta_0^{1+\nu_h/\nu_h} = (k_h^{1+\nu_h}/m)^{1/\nu_h}(c_h/\nu_h)$ (see (Neill et al., 2009)). Thus values obtained for β_0 (with the $\log(X_h) \sim \log(Z)$ regression) can be used to predict X_h^0 (daily microbial growth on humus in the control, whose corresponding observations have not been used so far): with the uncertainty surrounding β_0, the 95% confidence interval for X_h^0 ranges from 0.48 to 1.7 with a mean value of 0.87 mg CO_2 per kg soil per day. Mean observed values for X_h^0 vary with time and range from 0.75 to 1.4 with a mean value of 0.98 mg CO_2 per kg soil per day.

4. Discussion

In this paper, we compared two formalisms, the maximum caliber formalism and the extended mass action formalism, to model soil organic matter dynamics and priming effects in particular. Those formalisms were interesting to consider for a number of reasons: both are able to predict a priori the existence of priming effects, positive and negative. The maximum caliber formalism is appealing for its mathematical properties, its theoretical derivation and implications (Neill and Gignoux, 2008; Neill et al., 2009), whereas the extended mass action formalism has the advantage to generalize a number of well-known formalisms. We constructed a model using a simple soil representation and either of the two formalisms. The 5 compartment soil representation used here is a simplification of reality and this induced some limitations as discussed in the methods section. However, as the two formalisms were applied on the same model structure their relative performance could not be attributed to structure limitations. Furthermore the main shortcoming of our model structure was the assumption of litter homogeneity and the ensuing constancy of k_l, while the ramifications of our results discussed below do not depend on k_l.

We showed with simple calculations that the relationship between two fluxes, namely microbial growth on humus, x_h, and microbial mortality, z, differed between the two formalisms, and we used a substantial data set to test these contrasted predictions. Our test supported the MAXCAL formalism over the EMA one.

To what extent does this relationship matter in determining the priming effect intensity or more generally the behaviour of a soil system?

In and of itself the relationship between x_h and z does not suffice to determine the priming intensity in general, since, from eqs. (12), (13) and (14), x_h and z (and x_l as well) are mutually dependent. That is, z cannot be calculated from the state variables c_h, c_l, n and b independently of x_h. This relationship does suffice to determine the priming effect intensity in one case of interest however: when mineral nitrogen and microbial biomass are both at quasi-steady state, i.e. $\delta n \approx 0$ and $\delta b \approx 0$. This case is likely informative of the asymptotic behaviour of the system if the added labelled substrate decomposes slowly enough (such as straw). In the experiment used here, we saw that mineral nitrogen was likely at steady state between days 15 and 67 of the incubations (Fig. 3). It is more difficult to ascertain whether microbial biomass was at steady state during the same time interval without any direct measurements. However our calculations of the three fluxes x_h, x_l and z incidentally show that microbial biomass was not quite at steady state within the 15–67 time interval, but not very far from it either (see Fig. 6 where it is shown that $x_h + x_l \geq z$ and thus δb positive).

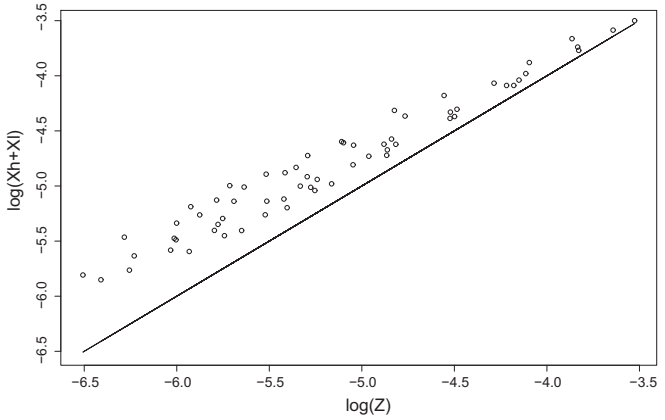

Fig. 6. Fluxes $\log(X_h + X_l)$ plotted against $\log(Z)$ (see text), all treatments pooled, for $\eta = 0.5$ and $n_b = 0.1$. Values correspond to fluxes expressed in g C per kg soil per day. The line is the 1:1 bisecting line.

Setting $\delta n = 0$ in eq. (4) yields:

$$(n_h\nu_h - n_b)x_h + (n_b - \eta n_h)z - (n_b - n_l\nu_l)x_l = 0$$

If we had in addition $\delta b = x_h + x_l - z \approx 0$, then

$$(n_h\nu_h - n_l\nu_l)x_h = (\eta n_h - \eta_l\nu_l)z$$

Using finally the relationship $x_h = \beta_0 z^{\beta_1}$:

$$(n_h\nu_h - n_l\nu_l)x_h = (\eta n_h - n_l\nu_l)\left(\frac{x_h}{\beta_0}\right)^{1/\beta_1} \quad (15)$$

If $\beta_1 = 1$ as predicted by the EMA formalism, x_h cancels out from eq. (15), which then has no solution except for a very particular set of parameters. This means that in most cases, there is no simultaneous steady state for mineral nitrogen and microbial biomass in a system governed by the EMA formalism.

Much more likely is that, as predicted by the MAXCAL formalism, $\beta_1 = (1/1 + \nu_h)$. Then a steady state for mineral nitrogen and microbial biomass is always feasible if $\eta n_h > n_l\nu_l$ (i.e. if less nitrogen is provided in the litter than is required for humification) and eq. (15) sets the value of x_h:

$$x_h^{\nu_h} = \beta_0^{1+\nu_h}\frac{(n_h\nu_h - n_l\nu_l)}{(\eta n_h - n_l\nu_l)} \quad (16)$$

Therefore the value of β_1 affects the feasibility of steady states and this could have consequences for the medium to long-term behaviour of the whole system.

With regards to the priming effect intensity, eq. (16) can be interpreted in a meaningful way. Eq. (16) can be rewritten using x_h^0 (introduced in the results section as x_h in the control) as:

$$\frac{x_h}{x_h^0} = \left(\frac{n_h\nu_h - n_l\nu_l}{\eta n_h - n_l\nu_l}\right)^{1/\nu_h} \quad (17)$$

The ratio x_h/x_h^0 is a way to quantify the priming effect in terms of a proportional change rather than an incremental one. Eq. (17) above says that, at quasi-steady state for mineral nitrogen and microbial biomass in a soil system, the priming effect will: i) be "positive" (i.e. $x_h > x_h^0$) since $n_h\nu_h - n_l\nu_l > \eta n_h - n_l\nu_l$. It is generally observed that "negative" priming effects ($x_h > x_h^0$) are only transient phenomena and that ultimately they become positive (Blagodatskaya and Kuzyakov, 2008); ii) depend only on stoichiometric parameters, not kinetic ones; iii) increases with the difference $n_h\nu_h - n_l\nu_l$, which is the difference of nitrogen supply between humus and litter; the more nitrogen humus is likely to provide, the

higher the priming: this is consistent with the microbial nitrogen mining hypothesis (Moorhead and Sinsabaugh, 2006; Craine et al., 2007); iv) but priming also decreases with the difference $\eta n_h - n_l \nu_l$, which is the amount of nitrogen required in addition to the nitrogen supplied by litter to humify ν_l units of litter carbon. Let us call it the litter humification nitrogen demand. This might seem contradictory with iii). Yet it is logical as well in that it reflects the overall process rate limitations induced by nitrogen deficiency (see below that at steady state for mineral nitrogen and microbial biomass, litter decomposition rate is proportional to humus decomposition rate). This is consistent with basic stoichiometric decomposition theory. The model combines the two mechanisms iii) and iv) to predict that priming intensity will be an increasing function of $n_l \nu_l$, the litter nitrogen "offer".

We also note that in eq. (17), the microbial C:N ratio does not affect the priming intensity, nor does the amount of mineral nitrogen available. The parameter n_b (the microbial N:C ratio) disappeared from the calculus above when we assumed microbial biomass was at steady state. This is logic: when microbial biomass is at steady state, it behaves as a pipe, and does not immobilize nor remineralize nitrogen. Its C:N ratio thus becomes indifferent to the dynamics of the system. This goes against previous views on the role of microbial stoichiometry in soil organic matter dynamics (Fontaine et al., 2003; Sinsabaugh et al., 2009). Fontaine et al. for instance, argued that microbial competition should regulate priming intensity through shifts in the community-level microbial C:N ratio.

Similarly, when mineral nitrogen is at steady state, it does not affect the dynamics of the system any more, and its actual availability becomes indifferent. These two observations might explain why, in the experiment analyzed here, mineral nitrogen additions had little effect on the priming intensity. Indeed, adding mineral nitrogen had two consequences: the microbial C:N ratio decreased and mineral nitrogen availability increased. As we have just seen, neither of these changes should be expected to alter the priming intensity at quasi-steady state for microbes and mineral nitrogen.

It is important to realize that these results are not built in the assumptions of the MAXCAL formalism. They arise as a consequence of the dynamics of the system, when all the state variables have had time to adjust to one another. On an "instantaneous" basis, mineral nitrogen availability and microbial C:N ratio do affect litter and humus mineralization rates, as is evident from the fact that they appear in eq. (13) and that eqs. (12)–(14) are coupled.

Finally we point out that in a model where all the fluxes are mutually dependent, knowing x_h suffices to determine x_l as well at steady state for mineral nitrogen and microbial biomass. One has then:

$$(\eta n_h - n_l \nu_l) x_l = n_h (\nu_h - \eta) x_h$$

which says that x_l adjusts so that the nitrogen provided by humus mineralization compensates exactly the litter humification nitrogen demand. Again neither the availability of mineral nitrogen nor n_b appear in this equation. This might explain why studies that have added mineral nitrogen show inconsistent effects on decomposition, with a number of them showing little effect on litter decomposition (Hobbie, 2005, 2008, and references therein), including the data used here. This also suggests that the critical litter C:N ratio above which litter decomposition is nitrogen limited is $\nu_l/\eta n_h$ instead of ν_l/n_b. This could shed a new light on results such as those of Manzoni et al. (2008) for instance. Manzoni et al. used simple mass balance equations to analyze an extensive data base of litter decomposition rates. However in their equations they did not account for microbial nitrogen remineralization and thus interpreted measured critical ratios as ν_l/n_b ($1/er_b$, in their notation, with e carbon use efficiency and r_b microbial N:C ratio). After they assigned a value of 0.1 to n_b (r_b), they concluded that carbon use efficiencies $e = 1/\nu_l$ where lower than generally assumed (between 0.1 and 0.3 from their Fig. 3). Had they interpreted the measured critical ratios in terms of $\nu_l/\eta n_h$ and assigned a plausible value of $0.5 \times 0.1 = 0.05$ to the denominator, they would have found carbon use efficiencies between 0.2 and 0.6, more in line with in vitro incubation studies measurements.

4.1. Conclusions

Two formalisms, the maximum caliber and the extended mass action formalisms, were applied to a common soil compartimentation scheme and their predictions confronted with a non trivial set of priming observations. We acknowledged the limitations of our simple model structure, particularly the difficulty to simulate litter decomposition kinetics with a single litter pool. But we showed that the two formalisms generated distinct, testable predictions and that the maximum caliber formalism agreed with the observations whereas the extended mass action formalism was at odds with them. We discussed the determinants of priming effect intensity as predicted by the maximum caliber formalism. Based on our findings, we advocate for the quantification of the priming effect as a ratio rather than a difference. We also encourage studies of priming effects with complex substrates, decomposing slowly enough so that mineral nitrogen and microbial biomass may reach quasi-steady states and the predictions of eq. (17) tested more thoroughly.

Acknowledgements

We thank Naoise Nunan and Clive G. Jones for helpful comments on this manuscript. This work was supported by the Ecole des Mines de Paris, Chaire Nouvelles Stratégies Energétiques and the Région Ile de France via the R2DS funding program. Neither funding sources took any part in the achievement of this work.

Appendix

Negative and positive priming in the maximum caliber formalism

Let us show using eqs. (12), (13) and (14) that $\partial x_h/\partial c_l \leq 0$ (negative priming because of substrate competition) and $\partial x_h/\partial b \geq 0$ (positive priming because of biomass increase). Taking the logarithm of eq. (12), we have:

$$\log(x_h) = \log(k_h) + \frac{1}{1+\nu_h}\log\left(\widehat{b}\right) + \frac{\nu_h}{1+\nu_h}\log\left(\widehat{c}_h\right) \tag{18}$$

where $\widehat{b} = b - x_h - x_l - z = \frac{z}{m} = \frac{1}{1+m}(b - x_h - x_l)$ from eq. (14) and $\widehat{c}_h = (c_h - \nu_h x_h/\nu_h)$. Similarly, from eq. (13), we have:

$$\log(x_l) = \log(k_l) + \frac{1}{1+\nu_l+\nu_n}\log\left(\widehat{b}\right) + \frac{\nu_l}{1+\nu_l+\nu_n}\log\left(\widehat{c}_l\right) + \frac{\nu_n}{1+\nu_l+\nu_n}\log\left(\widehat{n}\right) \tag{19}$$

with $\widehat{c}_l = (c_l - \nu_l x_l/\nu_l)$ and $\widehat{n} = (n - \nu_n x_l/\nu_n)$. Derivating 18 and 19 with respect to c_l yields:

$$\frac{1}{x_h}\frac{\partial x_h}{\partial c_l} = -\frac{1}{1+\nu_h}\frac{1}{\widehat{b}}\frac{1}{1+m}\left(\frac{\partial(x_h+x_l)}{\partial c_l}\right) - \frac{\nu_h}{1+\nu_h}\frac{1}{\widehat{c}_h}\frac{\partial x_h}{\partial c_l}$$

$$\frac{1}{x_l}\frac{\partial x_l}{\partial c_l} = -\frac{1}{1+\nu_l+\nu_n}\frac{1}{\widehat{b}}\frac{1}{1+m}\left(\frac{\partial(x_h+x_l)}{\partial c_l}\right) + \frac{\nu_l}{1+\nu_l+\nu_n}\frac{1}{\widehat{c}_l}\left(\frac{1}{\nu_l} - \frac{\partial x_l}{\partial c_l}\right) - \frac{\nu_n}{1+\nu_l+\nu_n}\frac{1}{\widehat{n}}\frac{\partial x_l}{\partial c_l}$$

These equations can be rewritten as:

$$\frac{\partial x_h}{\partial c_l} \propto -\frac{1}{1+\nu_h}\frac{1}{\widehat{b}}\frac{1}{1+m}\left(\frac{\partial(x_h+x_l)}{\partial c_l}\right) \tag{20}$$

$$\frac{\partial x_l}{\partial c_l} \propto -\frac{1}{1+\nu_l+\nu_n}\frac{1}{\widehat{b}}\frac{1}{1+m}\left(\frac{\partial(x_h+x_l)}{\partial c_l}\right)+\frac{\nu_l}{1+\nu_l+\nu_n}\frac{1}{\widehat{c}_l}\frac{1}{\nu_l} \tag{21}$$

Note that from the way the model is constructed, $\widehat{b}$, $\widehat{c}_h$, $\widehat{c}_l$ and $\widehat{n}$ are always positive.

Suppose now $\partial x_h/\partial c_l > 0$. Then from eq. (20), we deduce that $\partial(x_h+x_l)/\partial c_l < 0$ and from eq. (21), that $\partial x_l/\partial c_l > 0$. But then we must have $\partial(x_h+x_l)/\partial c_l > 0$. The contradiction proves $\partial x_h/\partial c_l \leq 0$.

Similarly, let us take the derivative of 19 and 18 with respect to b:

$$\frac{1}{x_h}\frac{\partial x_h}{\partial b} = \frac{1}{1+\nu_h}\frac{1}{\widehat{b}}\frac{1}{1+m}\left(1-\frac{\partial(x_h+x_l)}{\partial b}\right)-\frac{\nu_h}{1+\nu_h}\frac{1}{\widehat{c}_h}\frac{\partial x_h}{\partial b}$$

$$\frac{1}{x_l}\frac{\partial x_l}{\partial b} = \frac{1}{1+\nu_l+\nu_n}\frac{1}{\widehat{b}}\frac{1}{1+m}\left(1-\frac{\partial(x_h+x_l)}{\partial b}\right)-\frac{\nu_l}{1+\nu_l+\nu_n}\frac{1}{\widehat{c}_l} \times\frac{\partial x_l}{\partial b}-\frac{\nu_n}{1+\nu_l+\nu_n}\frac{1}{\widehat{n}}\frac{\partial x_l}{\partial b}$$

Suppose $(\partial x_h/\partial b) < 0$. Then we must have $1-(\partial(x_h+x_l))/(\partial b) < 0$ which results in $(\partial x_l/\partial b) < 0$. So $\partial((x_h+x_l))/(\partial b) < 0$ which contradicts $1-(\partial(x_h+x_l))/(\partial b) < 0$, proving that $(\partial x_h/\partial b) \geq 0$.

Computing n_b values in all treatments

Suppose we know n_b in the treatment C1N0 and η for all treatments. Using eqs. (7), (8), (3), (4), we can write the cumulated variations between days 0 and 15 for the model state variables:

$$\Delta^i b = X_h^i + X_l^i - Z^i$$

$$\Delta^i n = (n_h\nu_h - n_b)X_h^i + (n_b - \eta n_h)Z^i - (n_b - n_l\nu_l)X_l^i$$

$$\Delta^i w_{12} = (\nu_h - \eta)X_h^i$$

$$\Delta^i w_{13} = (\nu_l - 1)X_l^i + (1-\eta)\left(Z^i - X_h^i\right)$$

where capital letters refer to cumulated fluxes and the superscript i refers to the initial phase (days 0–15).

Substituting also $X_h^i + X_l^i - \Delta^i b$ for Z^i, we have:

$$\Delta^i n = n_h(\nu_h - \eta)X_h^i - (\eta n_h - n_l\nu_l)X_l^i - (n_b - \eta n_h)\Delta^i b \tag{22}$$

$$\Delta^i w_{12} = (\nu_h - \eta)X_h^i \tag{23}$$

$$\Delta^i w_{13} = (\nu_l - \eta)X_l^i - (1-\eta)\Delta^i b \tag{24}$$

If n_b is unknown, we have four unknowns and three equations, so we need an additional equation. To this end, we made the assumption that the following relationship $\Delta^i b = \alpha X_l^i$ held with a constant coefficient α across all treatments. This would be true if the gross biomass growth rate were constant from day 0 to day 15. If so, then irrespective of the formalism chosen (maximum caliber or extended mass action), we expect that when unlabelled biomass is at quasi-steady state, the dynamics of the labelled biomass follow an equation of the form $\delta b_l = aX_l^i - cb_l$. The solution of this equation at day 15 reads $\Delta^i b = \frac{aX_l^i}{c}(1-(1-c)^{t_s})$, with $t_s = 15/\delta t$, showing that $\Delta^i b/X_l^i$ is constant across treatments at day 15. Labelled biomass probably does not grow at constant pace during the first 15 days of the incubations, but this approximation seemed reasonable enough. α could be estimated from treatment C1N0 and the resulting relationship used henceforth to complete the n_b calculations in all other treatments. We checked that within the plausible intervals for η and n_b in C1N0, we would always have $n_b \geq \eta n_h$ in all treatments.

Parameter estimation with Bayesian posterior sampling

The algorithm for sampling the Bayesian posterior

$$\mathrm{p}(\beta, r/data) = \int_{\eta,\mathrm{n_b}} p(\beta,\ r/\eta, n_b,\ data)\mathrm{p}(\eta, \mathrm{n_b})d\eta dn_b$$

followed a number of steps :

1) draw values for η and n_b (in C1N0). To sample them adequately within their respective plausible intervals, we used the logit-transformed for η and the log-transformed for n_b and sampled those uniformly on their corresponding intervals.
2) compute n_b values for each treatment using the rationale above.
3) compute the X_h and Z values for all treatments between days 15 and 67 (7 values per treatment). Pool those values into a single data set (with a total of $n = 7 \times 9 = 63$ observations). Compute $\log(X_h)$ and $\log(Z)$.
4) compute Pearson's correlation coefficient $r = corr(\log(X_h), \log(Z))$.
5) sample the Bayesian posterior for the parameters of the linear regression of $\log(X_h) \sim \log(Z)$. Let y be the column vector of the $\log(X_h)$ and X the $(n \times 2)$ design matrix with first colum filled with ones and second column the vector of the $\log(Z)$. We wanted to estimate β in the standard regression problem

$$y_i = x_i\beta + \epsilon_i$$

with $\epsilon_i \sim N(0, \sigma^2)$. The ordinary least-square expression to estimate the coefficient vector β is:

$$\widehat{\beta} = (X^TX)^{-1}X^Ty$$

Using appropriate conjugate priors for β and σ, the Bayesian posterior for those parameters has the form:

$$p(\beta, \sigma^2/y, X) \propto (\sigma^2)^{-(n+\nu_0+p)/2}\exp\left(-\frac{1}{2\sigma^2}(\beta-\tilde{\beta})^T(X^TX+A)(\beta-\tilde{\beta})\right) \times \exp\left(-\frac{(\nu_0 s_0^2 + ns^2)}{2\sigma^2}\right)$$

with $\tilde{\beta} = (X^TX+A)^{-1}(X^TX\widehat{\beta} + A\overline{\beta})$, $s^2 = (1/n-2)(y-X\widehat{\beta})^T(y-X\widehat{\beta})$ and ν_0, p, A, $\overline{\beta}$ and s_0 prior hyperparameters. We chose those hyperparameters to give non-informative priors. The posterior could then be approximated with :

$$p(\beta, \sigma^2/y, X) \propto (\sigma^2)^{-n/2}\exp\left(-\frac{1}{2\sigma^2}(\beta-\widehat{\beta})^T(X^TX)(\beta-\widehat{\beta})\right) \times \exp\left(-\frac{ns^2}{2\sigma^2}\right)$$

To sample this posterior, we first drew σ^2 from $p(\sigma^2/\widehat{\beta},\ y,\ X)$, which is an inverse gamma distribution. Then we drew β from $p(\beta/\sigma^2,\ y,\ X)$ which is a normal distribution. A normal Gibbs sampling algorithm would require iterating those two steps a number of times.

References

Agren, G.I., Bosatta, E., 1996. Theoretical Ecosystem Ecology: Understanding Element Cycles. Cambridge University Press, Cambridge.

Beddington, J.R., 1975. Mutual interference between parasites and predators and its effect on searching efficiency. Journal of Animal Ecology 44, 331–340.

Blagodatskaya, E., Kuzyakov, Y., 2008. Mechanisms of real and apparent priming effects and their dependence on soil microbial biomass and community structure: critical review. Biology and Fertility of Soils 45, 115–131.

Cleveland, C.C., Liptzin, D., 2007. C: N:P stoichiometry in soil: is there a "Redfield ratio" for the microbial biomass? Biogeochemistry 85, 235–252.

Craine, J.M., Morrow, C., Fierer, N., 2007. Microbial nitrogen limitation increases decomposition. Ecology 88, 2105–2113.

Danger, M., Daufresne, T., Lucas, F., Pissard, S., Lacroix, G., 2008. Does liebig's law of the minimum scale up from species to communities? Oikos 117, 1741–1751.

DeAngelis, D.L., Goldstein, R.A., O'Neill, R.V., 1975. A model for trophic interactions. Ecology 56, 881–892.

Fontaine, S., Mariotti, A., Abbadie, L., 2003. The priming effect of organic matter: a question of microbial competition? Soil Biology and Biochemistry 35, 837–843.

Fontaine, S., Bardoux, G., Abbadie, L., Mariotti, A., 2004a. Carbon input to soil may decrease soil carbon content. Ecology Letters 7, 314–320.

Fontaine, S., Bardoux, G., Benest, D., Verdier, B., Mariotti, A., Abbadie, L., 2004b. Mechanisms of the priming effect in a savannah soil amended with cellulose. Soil Science Society of America Journal 68, 125–131.

Fontaine, S., Barot, S., Barre, P., Bidoui, N., Mary, B., Rumpel, C., 2007. Stability of organic carbon in deep soil layers controlled by fresh carbon supply. Nature 450, 277–280.

Guenet, B., Neill, C., Bardoux, G., Abbadie, L., Controls of organic matter input on priming effect. Soil Biology and Biochemistry, submitted for publication.

Guo, L.B., Gifford, R.M., 2002. Soil carbon stocks and land use change: a meta analysis. Global Change Biology 8, 345–360.

Hobbie, S.E., 2005. Contrasting effects of substrate and fertilizer nitrogen on the early stages of litter decomposition. Ecosystems 8, 644–656.

Hobbie, S.E., 2008. Nitrogen effects on decomposition: a five-year experiment in eight temperate sites. Ecology 89, 2633–2644.

Jaynes, E.T., 1985. Macroscopic prediction. In: Haken, H. (Ed.), Complex Systems – Operational Approaches in Neurobiology, Physics and Computers. Springer-Verlag, Berlin, pp. 254–269.

Kindler, R., Miltner, A., Richnow, H., Kastner, M., 2006. Fate of gram-negative bacterial biomass in soil – mineralization and contribution to som. Soil Biology and Biochemistry 38, 2860–2870.

Kuzyakov, Y., Friedel, J.K., Stahr, K., 2000. Review of mechanisms and quantification of priming effects. Soil Biology and Biochemistry 32, 1485–1498.

Lal, R., Kimble, J., Levine, E., Whitman, C., 1995. World soils and geenhouse effect: an overview. In: Lal, R., Kimble, J., Levine, E., Stewart, B.A. (Eds.), Soils and Global Change. CRC Press, Boca Raton, pp. 1–9.

Manzoni, S., Porporato, A., 2009. Soil carbon and nitrogen mineralization: theory and models across scales. Soil Biology and Biochemistry 41, 1355–1379.

Manzoni, S., Jackson, R.B., Trofymow, J.A., Porporato, A., 2008. The global stoichiometry of litter nitrogen mineralization. Science 321, 684–686.

Molina, J.A.E., 1996. Description of the Model NCSOIL. In: Powlson, D.S., Smith, P., Smith, J.U. (Eds.), Evaluation of Soil Organic Matter Models. Springer, Berlin, pp. 269–274.

Moorhead, D.L., Sinsabaugh, R.L., 2006. A theoretical model of litter decay and microbial interaction. Ecological Monographs 76, 151–174.

Neill, C., Gignoux, J., 2006. Soil organic matter dynamics driven by microbial growth: a simple model for a complex network of interactions. Soil Biology and Biochemistry 38, 803–811.

Neill, C., Gignoux, J., 2008. Prediction of non-equilibrium dynamics in ecosystems: from dogs and fleas to molecules and organisms. Journal of Statistical Mechanics: Theory and Experiment 1, P01001.

Neill, C., Daufresne, T., Jones, C.G., 2009. A competitive coexistence principle? Oikos 118, 1570–1578.

Nicolardot, B., Recous, S., Mary, B., 2001. Simulation of C and N mineralisation during crop residue decomposition: a simple dynamic model based on the C: N ratio of residues. Plant and Soil 83, 83–103.

Parton, W.J., Schimel, J.P., Cole, C.V., Ojima, D.S., 1987. Analysis of factors controlling soil organic-matter levels in great-plains grasslands. Soil Science Society of America Journal 51, 1173–1179.

Paul, E.A., Paustian, K., Elliott, E.T., Cole, C.V. (Eds.), 1997. Soil Organic Matter Dynamics in Temperate Agroecosystems. CRC Press, Boca Raton.

Saffih-Hdadi, K., Mary, B., 2008. Modeling consequences of straw residues export on soil organic carbon. Soil Biology and Biochemistry 40, 594–607.

Schlesinger, W.H., Andrews, J.A., 2000. Soil respiration and the global carbon cycle. Biogeochemistry 48, 7–20.

Sinsabaugh, R.L., Hill, B.H., Follstad Shah, J.J., 2009. Ecoenzymatic stoichiometry of microbial organic nutrient acquisition in soil and sediment. Nature 462, 795–798.

Sterner, R.W., Elser, J.J., 2002. Ecological Stoichiometry: the Biology of Elements from Molecules to the Biosphere. Princeton University Press, Princeton.